Cell, Vol. 90, 549–558, August 8, 1997, Copyright ©1997 by Cell Press

Huntingtin-Encoded Polyglutamine Expansions Form Amyloid-like Protein Aggregates In Vitro and In Vivo

Eberhard Scherzinger,* Rudi Lurz,*
Mark Turmaine,‡ Laura Mangiarini,†
Birgit Hollenbach,* Renate Hasenbank,*
Gillian P. Bates,† Stephen W. Davies,‡
Hans Lehrach,* and Erich E. Wanker*
*Max-Planck-Institut für Molekulare Genetik
D-14195 Berlin (Dahlem)
Germany
†Division of Medical and Molecular Genetics
United Medical and Dental Schools
Guy's Hospital
London SE1 7EH
United Kingdom
‡Department of Anatomy and Developmental Biology
University College London
London WC1E6BT
United Kingdom

Summary

The mechanism by which an elongated polyglutamine sequence causes neurodegeneration in Huntington's disease (HD) is unknown. In this study, we show that the proteolytic cleavage of a GST-huntingtin fusion protein leads to the formation of insoluble high molecular weight protein aggregates only when the polyglutamine expansion is in the pathogenic range. Electron micrographs of these aggregates revealed a fibrillar or ribbon-like morphology, reminiscent of scrapie prions and β-amyloid fibrils in Alzheimer's disease. Subcellular fractionation and ultrastructural techniques showed the in vivo presence of these structures in the brains of mice transgenic for the HD mutation. Our in vitro model will aid in an eventual understanding of the molecular pathology of HD and the development of preventative strategies.

Introduction

Huntington's disease (HD) is an autosomal dominant progressive neurodegenerative disorder characterized by personality changes, motor impairment and subcortical dementia (Harper, 1991). It is associated with a selective neuronal cell death occurring primarily in the cortex and striatum (Vonsattel et al., 1985). The disorder is caused by a CAG/polyglutamine (polygln) repeat expansion in the first exon of a gene encoding a large ~350 kDa protein of unknown function (Huntington's Disease Collaborative Research Group, 1993). The CAG repeat is highly polymorphic and varies from 6 to 39 repeats on chromosomes of unaffected individuals and from 36 to 180 repeats on *HD* chromosomes (Rubinsztein et al., 1996; Sathasivam et al., 1997). The majority of adult onset cases have expansions ranging from 40 to 55 units, whereas expansions of 70 and above invariably cause the juvenile form of the disease. The normal and mutant forms of huntingtin have been shown to be expressed at similar levels in the central nervous system and are also present in peripheral tissues (Trottier et al., 1995a). Within the brain, huntingtin was found predominantly in neurons and was present in cell bodies, dentrites, and also in the nerve terminals. Immunohistochemistry, electron microscopy, and subcellular fractionations have shown that huntingtin is primarily a cytosolic protein, a fraction of which is associated with vesicles and/or microtubules, suggesting that it plays a functional role in cytoskeletal anchoring or transport of vesicles (DiFiglia et al., 1995; Gutekunst et al., 1995; Sharp et al., 1995) Huntingtin has also been detected in the nucleus (Hoogeveen et al., 1993; de Rooij et al., 1996), suggesting that transcriptional regulation cannot be ruled out as a possible function of this protein.

In addition to HD, CAG/polygln expansions have been found in at least six other inherited neurodegenerative disorders including spinal and bulbar muscular atrophy (SBMA), dentatorubral pallidoluysian atrophy (DRPLA), and the spinocerebellar ataxia (SCA) types 1, 2, 3, and 6 (referenced in Bates et al., 1997). The normal and expanded size ranges are comparable with the exception of SCA6 in which the expanded alleles are smaller and the mutation is likely to act by a different route. However, in all cases the CAG repeat is located within the coding region and is translated into a stretch of polygln residues. Although the proteins harboring the polygln sequences are unrelated and mostly of unknown function, it is likely that the mutations act through a similar mechanism. Without exception, these proteins are widely expressed and generally localized to the cytoplasm. However, despite overlapping expression patterns in brain, the neuronal cell death is relatively specific and can differ markedly (Ross, 1995), indicating that additional factors are needed to convey the specific patterns of neurodegeneration.

Several investigators have proposed that HD is caused by a toxic gain of function, which in turn is caused by abnormal protein–protein interactions related to the elongated polygln. It is possible that the binding of a protein to the polygln region could either confer a new property on huntingtin or alter its normal interactions, causing selective cell death either through the specific expression patterns of the interacting protein or through the selective vulnerability of certain cells. To date, four potential huntingtin-interacting proteins have been isolated: HAP1 (Li et al., 1995), GAPDH (Burke et al., 1996), HIP2 (Kalchman et al., 1996), and HIP-I (Kalchman et al., 1997; Wanker et al., 1997). However, an involvement of these proteins in the selective neuropathology has not been demonstrated. A gain-of-function mechanism has been supported by the identification of an antibody that specifically reacts with the pathogenic polygln expansions (Trottier et al., 1995b). This indicates that upon expansion into the pathogenic range, a polygln sequence may undergo a conformational change. Poly-L-glutamines form pleated sheets of β strands held together by hydrogen bonds between their amides (Perutz et al., 1994). It was proposed that

the expanded glutamine repeats in huntingtin may function as polar zippers, joining protein molecules together (Perutz, 1996). In the long run, this could result in the precipitation of huntingtin protein in specific neurons, causing the observed selective neuronal loss. Thus, the mechanism underlying HD would be similar to scrapie, Creutzfeldt-Jakob, or Alzheimer's disease, in which β-sheet secondary structures lead to the formation of toxic protein aggregates in selective neurons (Caughey and Chesebro, 1997).

Recently, lines of mice (R6) that are transgenic for the HD mutation have been generated (Mangiarini et al., 1996). In these mice, exon 1 of the human *HD* gene carrying CAG repeat expansions of 115–156 units is expressed under the control of the human HD promoter. It has been demonstrated that the transgenic animals exhibit a progressive neurological phenotype that exhibits many of the motor and nonmotor features of HD. The phenotype includes a resting tremor; irregular gait; rapid, abrupt shuddering movements; stereotypic grooming movements; and epileptic seizures. Coincident with the onset of the movement disorder, the mice show a progressive weight loss. Neuropathological analysis has shown a reduction in brain weight (which precedes that in body weight) and the presence of neuronal intranuclear inclusions (NIIs) predating any evidence of neuronal dysfunction (Davies et al., 1997 [this issue of *Cell*]). The NIIs are immunoreactive for N-terminal huntingtin antibodies that detect the transgene protein and for ubiquitin but do not contain the endogenous mouse huntingtin. At the ultrastructural level, a solitary intranuclear inclusion appears as a roughly circular pale structure of a fine granular nature with occasional filamentous structures and devoid of a membrane. In addition, the neurons invariably have indentations of the nuclear membrane and an apparent increase in the density and clustering of nuclear pores. All three of these ultrastructural nuclear changes have previously been reported in EM studies from HD patients (Tellez-Nagel et al., 1974; Roizin et al., 1979; Roos and Bots, 1983).

In this report, we have used exon 1 of the *HD* gene with expanded CAG repeats for the production of glutathione S-transferase (GST)-HD fusion proteins in E. coli. The recombinant proteins were purified under native conditions by affinity chromatography (Smith and Johnson, 1988). Site-specific proteolysis of a GST-HD51 fusion protein with a polygln expansion in the pathological range (51 glutamines) resulted in the formation of high molecular weight protein aggregates with a fibrillar or ribbon-like morphology. The filaments, which were not produced by proteolysis of shorter fusion proteins (20 or 30 glutamines), were similar to scrapie prions and β-amyloid-like fibrils in Alzheimer's disease, and also resemble those detected by electron microscopy in the NIIs of mice trangenic for the HD mutation.

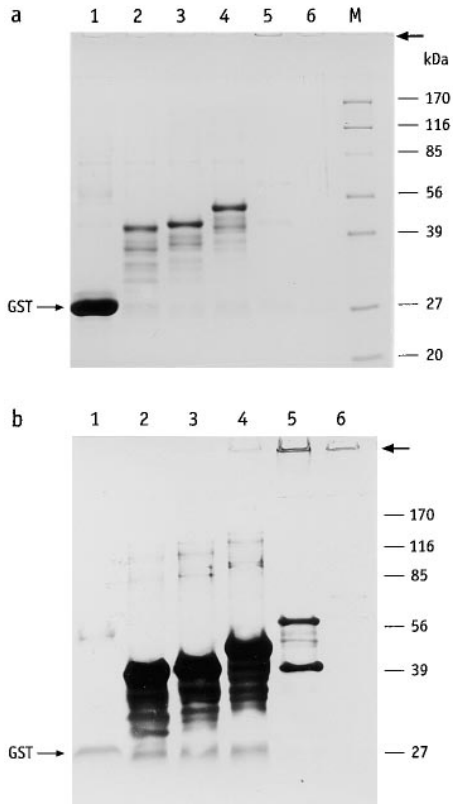

Figure 1. SDS–PAGE Analysis of Purified GST and GST-HD Fusion Proteins

(a) Aliquots (15 μl) of eluates from the glutathione agarose column were subjected to 12.5% SDS–PAGE and analyzed by staining with Coomassie blue R. Lanes 1–6 contain GST, GST-HD20, -HD30, -HD51, -HD83, and -HD122, respectively; lane M contains molecular mass standards.

(b) Proteins were transferred to nitrocellulose and probed with anti-HD1 antibody. Arrows mark the origin of electrophoresis.

Results

Purification of GST-HD Fusion Proteins Containing Expanded Polyglns

Exon 1 of the *HD* gene was isolated from genomic phage clones, derived from the normal and expanded alleles of an HD patient (Sathasivam et al., 1997), and used for the expression of GST-HD fusion proteins in E. coli. DNA fragments containing CAG repeats in the normal $(CAG)_{20–33}$ and expanded $(CAG)_{37–130}$ range were cloned into pGEX-5X-1 (Pharmacia), and the resulting plasmids expressing fusion proteins with 20 (GST-HD20), 30 (-HD30), 51 (-HD51), 83 (-HD83), and 122 (-HD122) glutamines, respectively, were used for protein purification. After induction with IPTG, the resulting proteins were purified under native conditions by affinity chromatography on glutathione agarose. SDS–PAGE of the purified GST-HD20, -HD30, -HD51, -HD83, and -HD122 proteins revealed major bands of 42, 45, 50, 65, and 75 kDa, respectively (Figure 1a). These bands were also detected when the various protein fractions were subjected to immunoblot analysis using the affinity-purified anti-huntingtin antibody HD1 (Figure 1b, lanes 2–6). HD1 specifically detects the GST-HD fusion proteins on immunoblots, whereas the GST tag alone is not recognized (Figure 1b, lane 1). All recombinant proteins migrated at a size corresponding nearly to that predicted from their amino acid sequence. Interestingly, an additional high molecular weight band that remains at the top of the gel was consistently detected in the protein fractions with the longest polyglns (83 and 122 residues; Figures

Figure 2. Structure of GST-HD Fusion Proteins

The amino acid sequence corresponding to exon 1 of huntingtin is boxed. Arrows labeled (Xa) and (T) indicate cleavage sites for factor Xa and trypsin, respectively.

1a and 1b, lanes 5 and 6). This band was most prominent on the immunoblots but was also clearly detectable in the Coomassie-stained gel. This immunoreactive material was often still present at the bottom of the loading slots, even after the samples had been boiled for 5 min in the presence of 2% SDS and 6 M urea prior to loading.

Proteolytic Cleavage of GST-HD Fusion Proteins Containing Expanded Polyglns

It has been shown previously that the solubility of certain proteins can be enhanced by the addition of the GST tag (Smith and Johnson, 1988), and it was therefore of interest to determine whether the removal of the GST tag by proteolytic cleavage would have an effect on the solubility of the polygln-containing fusion proteins. Potential factor Xa and trypsin cleavage sites within the GST-HD fusion proteins are shown in Figure 2. Factor Xa cleaves between the GST tag and the HD exon 1 protein, whereas trypsin removes an additional 15 amino acids from the N terminus and a single proline from the C terminus, both proteases leaving the polygln repeat intact. The GST-HD20, -HD30, and -HD51 proteins were digested with trypsin under conditions designed to remove the GST tag from the fusion protein without it being totally degraded. After cleavage, proteins were denatured by boiling in the presence of 2% SDS and analyzed by SDS–PAGE and immunoblotting using the anti-HD1 antibody. GST-HD20 and -HD30 cleavage yielded products migrating in a 12.5% gel at approximately 30 and 33 kDa, respectively. In contrast, cleavage of GST-HD51 resulted in the formation of two protein products migrating at approximately 37 and 60 kDa, and an additional weak immunoreactive band on the bottom of the loading slots was also detected (Figure 3a). This high molecular weight band was more pronounced when GST-HD51 was digested with trypsin under conditions in which the GST tag was totally degraded (Figure 3b). However, with proteins GST-HD20 and -HD30, this longer exposure to trypsin produced the same cleavage products as the ones seen in Figure 3a, and the high molecular weight products were not observed. Similar results were obtained with factor Xa protease and endoproteinases Arg-C and Lys-C (data not shown).

We have developed a simple and sensitive filter assay to detect the formation of high molecular weight insoluble protein aggregates. This assay is based on the finding that the SDS-insoluble protein aggregates obtained by proteolytic cleavage of GST-HD51 are retained on a cellulose acetate filter, whereas the soluble cleavage products of GST-HD20 and GST-HD30 are not. Figure 3c shows immunoblots of cellulose acetate and nitrocellulose membranes to which the native GST-HD20, -HD30, and -HD51 proteins and their factor Xa and trypsin cleavage products have been applied. On the cellulose acetate filter, only the cleavage products of GST-HD51 were detected by the anti-HD1 antibody, indicating the formation of insoluble high molecular weight protein aggregates. In contrast, all of the uncleaved GST-HD fusion proteins and their digestion products were detected on the nitrocellulose control filter.

Huntingtin Proteins Containing Expanded Polyglns in the Pathological Range Aggregate to Amyloid-Like Birefringent Fibrils

Electron microscopy of negatively stained GST-HD51 fractions showed oligomeric particles with diameters of 6–7 nm (Figure 4a); no higher ordered aggregates were observed. In contrast, protein fractions obtained by proteolytic cleavage of GST-HD51 showed numerous clusters of high molecular weight fibrils and ribbon-like structures (Figures 4b–4e), reminiscent of purified amyloids (Prusiner et al., 1983). The fibrils obtained after digestion with factor Xa showed a diameter of 10–12 nm, and their length varied from 100 nm up to several micrometers (Figures 4b and 4c). In the trypsin-treated samples, ribbon-like structures formed by lateral aggregation of fibrils with a diameter of 7.7 nm were observed (Figures 4d and 4e). After treatment with factor Xa or limited digestion with trypsin, clots of small particles were frequently detected on one or both ends of the fibrils (Figures 4b–4d). These clots of varying sizes and shapes were not seen when GST-HD51 was digested with trypsin under conditions in which the GST tag is totally degraded (Figure 4e), indicating that they contain GST. In strong contrast to GST-HD51, the GST-HD20 and -HD30 proteins did not show any tendency to form ordered high molecular weight structures, either with or without protease treatment (Figure 4f).

The insoluble protein aggregates formed by proteolytic cleavage of GST-HD51 were isolated by centrifugation and stained with Congo red (Caputo et al., 1992). After staining, the protein aggregates on the glass slides were red, indicating that they had bound the dye (Figure 5a), and when examined under polarized light, a green color and birefringence were detected (Figures 5b and 5c). These staining characteristics were similar to those observed for prions (Prusiner et al., 1983) and amyloids (Caputo et al., 1992).

Huntingtin Proteins Containing Expanded Polyglns Form Amyloid-Like Protein Aggregates In Vivo

To determine whether the amyloid-like protein aggregates formed by proteolytic cleavage of GST-HD51 in vitro are also present in vivo, nuclear protein fractions of brain and kidney were prepared from mice transgenic

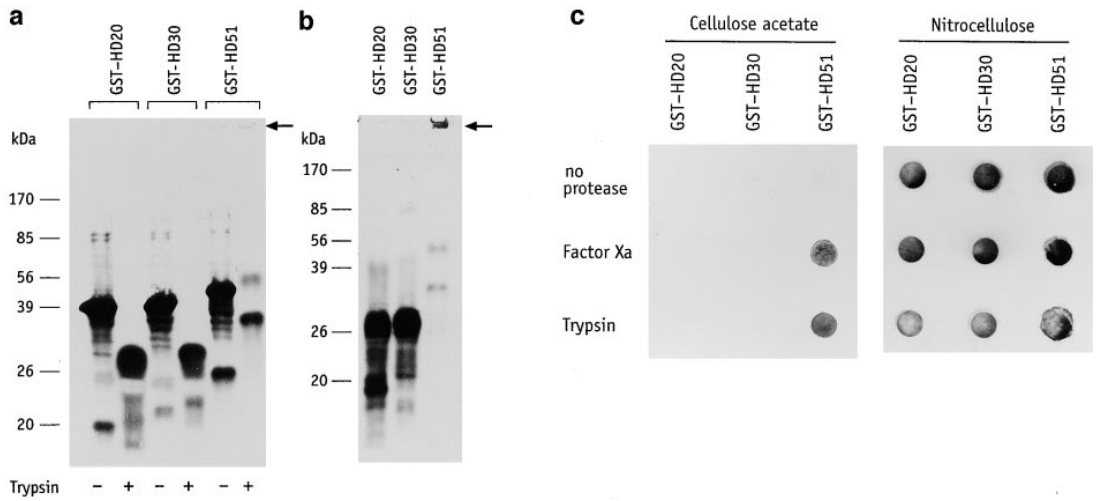

Figure 3. Site-Specific Proteolysis of GST-HD Fusion Proteins with Trypsin and Factor Xa

(a and b) Tryptic digestions were performed at 37°C for 3 (a) or 16 hr (b). Native proteins and their cleavage products were subjected to 12.5% SDS–PAGE, blotted onto nitrocellulose membranes, and probed with anti-HD1 antibody. Arrows mark the origin of electrophoresis.

(c) Purified fusion proteins and their factor Xa and trypsin cleavage products were analyzed using the filter retardation assay. The proteins retained by the cellulose acetate and nitrocellulose membranes were detected by incubation with the anti-HD1 antibody.

for the HD mutation (line R6/2) and littermate controls (Mangiarini et al., 1996; Davies et al., 1997). The protein extracts were analyzed by SDS–PAGE and Western blotting using the anti-HD1 antibody (Figure 6a). Strikingly, this antibody detected a prominent high molecular weight band in the nuclear fraction (N) prepared from R6/2 transgenic brain, very similar to the high molecular weight band obtained by proteolytic cleavage of GST-HD51 (Figure 3b). No such immunoreactive band was detected in the nuclear fraction of brain from the littermate control, and it was also absent from the corresponding cytoplasmic fractions (C). A small amount of high molecular weight material was also detected in the nuclear fraction prepared from R6/2 transgenic kidney, but was again absent from the cytoplasmic fraction. The purity of the nuclear and cytoplasmic fractions was confirmed by Western blot analysis using the anti-Fos B and anti-GAPDH antibodies. Anti-Fos B detected the transcription factor mainly in the nuclear fraction, and the enzyme GAPDH was only seen in the cytoplasmic fraction, as expected. The Western blot results were reproduced using the cellulose acetate filter assay (Figure 6b). Using this assay, a 10- to 20-fold higher amount of transgene protein was detected in the nuclear fraction isolated from brain material, compared to that prepared from kidney.

The formation of NIIs has been shown to precede the neuronal dysfunction that forms the basis of the progressive neurological phenotype observed in the R6 transgenic lines (Davies et al., 1997). These NIIs are immunoreactive for both huntingtin and ubiquitin antibodies and contain the transgene but not the endogenous huntingtin protein. Therefore, Western blot analysis using an anti-ubiquitin antibody was also performed showing the same pattern of immunoreactivity as had been observed with the anti-HD1 antibody (Figure 6a), and indicating that the high molecular weight transgene protein present in the nuclear fraction is ubiquitinated (data not shown).

To examine whether the NIIs containing the proteins huntingtin and ubiquitin (Davies et al., 1997) have a fibrous composition, an ultrastructural analysis was performed. An electron micrograph of a NII from a 17 month old R6/5 homozygous mouse is shown in Figure 6c. This NII (large arrow) contains high molecular weight fibrous structures that were clearly differentiated from the surrounding chromatin. The filaments were randomly oriented, 5–10 nm in diameter, and often measured up to 250 nm in length (small arrows). These structures differ from those previously reported in the NIIs seen in hemizygous R6/2 mice that were far more granular in composition, with individual filamentous structures being more difficult to distinguish (Davies et al., 1997). R6/2 mice exhibit an earlier age of onset with a more rapid progression of the phenotype and do not survive beyond 13 weeks (Mangiarini et al., 1996). It is possible that the filamentous structures do not have time to form in the R6/2 mice.

Discussion

We have developed an in vitro system by which highly stable amyloid-like protein aggregates can be formed under defined conditions by proteolytic cleavage of GST fusion proteins corresponding to exon 1 of the *HD* gene and containing expanded polygln sequences. The arrays of fibrillar structures of varying sizes and shapes observed by electron microscopy clearly resemble those of purified amyloids. Furthermore, the polarization microscopic properties of the fibrils stained with Congo red are strikingly similar to those described for amyloids. The green-gold birefringence of the amyloid-like fibrils indicates that the polymers have common structural features. Although the Congo red staining does not determine conclusively whether the fibrils consist of β-pleated sheets, the method suggests that this is likely in view of experience gained with other protein polymers (Caputo et al., 1992). However, it has been generally

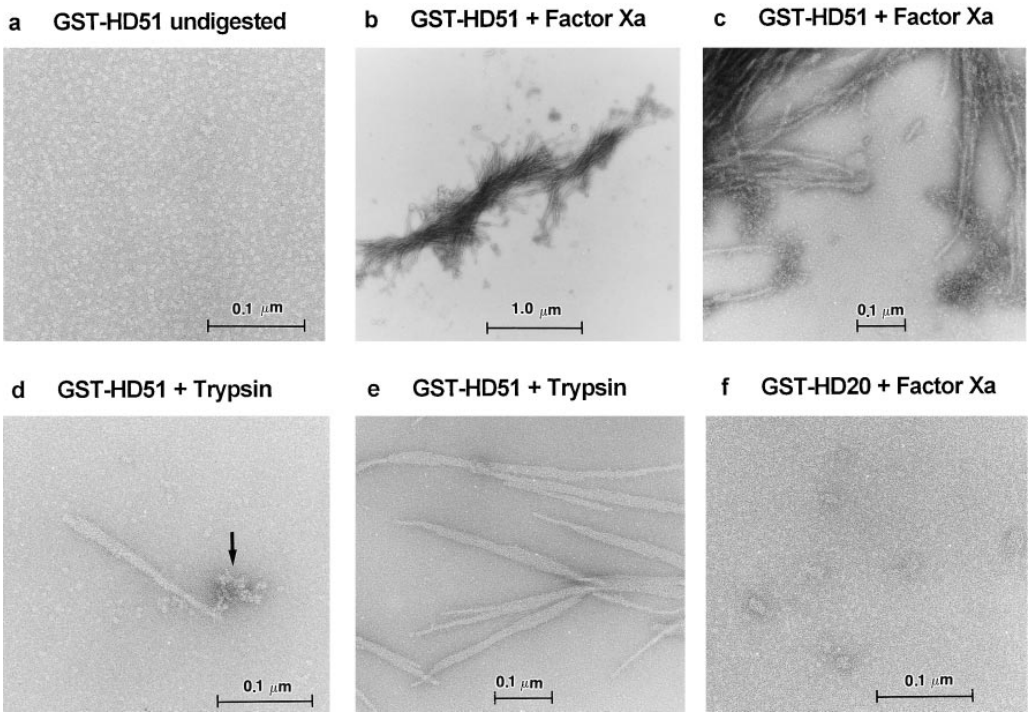

Figure 4. Electron Micrographs of Native GST-HD Fusion Proteins and Their Factor Xa and Trypsin Cleavage Products

Purified GST fusion proteins were protease treated, negatively stained with uranyl acetate, and viewed by electron microscopy. The undigested GST-HD51 molecules appear as a homogeneous population of small, round particles (a). Removal of the GST tag with factor Xa results in the formation of amyloid-like fibrils and intermediate structures (b and c). After partial digestion (3 hr) of GST-HD51 with trypsin, the ribbons are associated with terminal clots ([d], arrow), whereas prolonged digestion (16 hr) produces ribbons without attached clots (e). Removal of the GST tag from GST-HD20 shows no evidence for the formation of defined structures (f).

accepted that naturally occuring mammalian protein polymers that exhibit fibrillar structures and green birefringence after Congo red staining should be classified as amyloids (Glenner, 1980).

It has been shown by X-ray diffraction studies that synthetic peptides containing polygln s form β sheets strongly held together by hydrogen bonds (Perutz et al., 1994). Because synthetic poly(L-glutamine) is insoluble in water, a synthetic peptide with the sequence Asp_2-Gln_{15}-Lys_2 was used in that study. A stretch of 10 glutamines was also inserted into the loop of chymotrypsin inhibitor-2 (CI2), and it was demonstrated by analytical ultracentrifugation that the recombinant protein, in addition to monomers, formed dimers and trimers, whereas wild-type CI2 was present only in the monomeric form (Stott et al., 1995). It has been proposed that the polygln stretch functions as a polar zipper, joining proteins together. However, the hypothesis that glutamine repeats in proteins form β-pleated sheets and induce protein aggregation by a mechanism similar to that observed in spongiform encephalopathy (TSE) diseases (Caughey and Chesebro, 1997) could not be proven with this recombinant protein. Most likely, the length of the polygln sequence inserted into CI2 was too short.

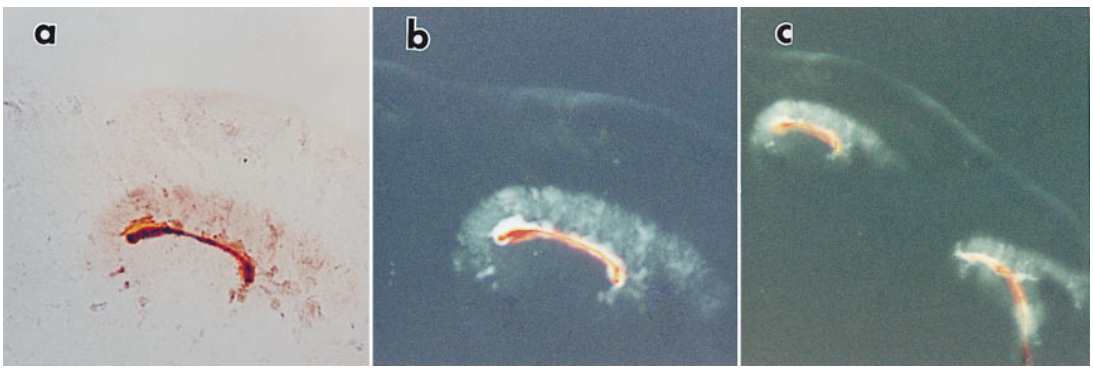

Figure 5. Birefringence of Protein Aggregates Formed by Proteolytic Cleavage of GST-HD51

The protein aggregates were stained with Congo red. (a) Bright field, 200×; (b) Polarized light, 200×; (c) Polarized light, 100×.

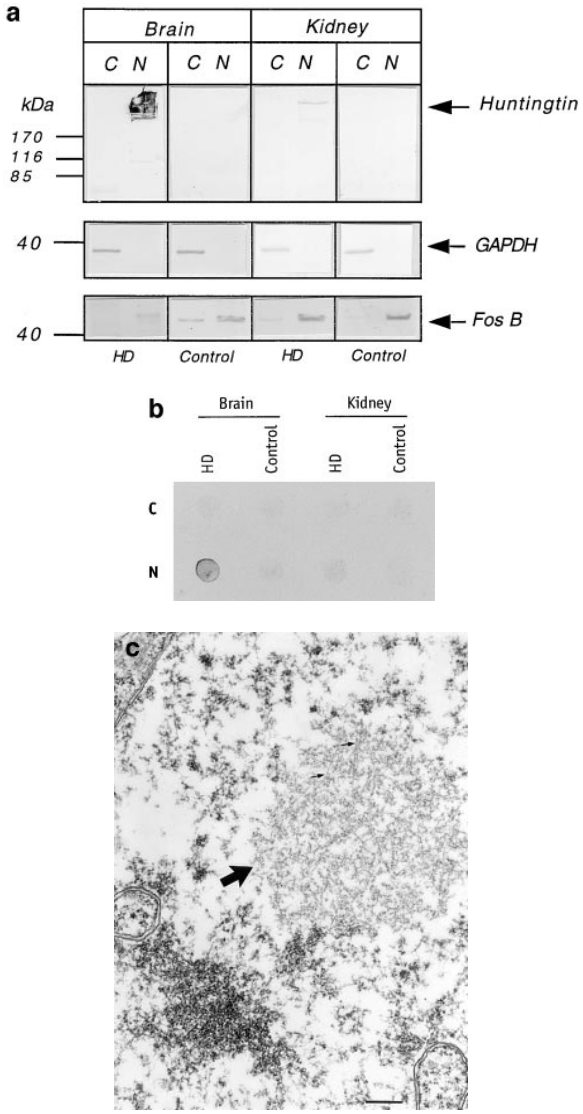

Figure 6. Polygln-Containing Protein Aggregates Are Formed In Vivo

(a) Western blot analysis, after separation by 10% SDS–PAGE, of the nuclear (N) and cytosolic (C) protein fractions prepared from brain and kidney of an R6/2 hemizygous transgenic mouse and a littermate control. Blots were probed with anti-HD1, anti-GAPDH, and anti-Fos B antibodies as indicated.

(b) Detection of HD exon 1 protein aggregates formed in vivo using the cellulose acetate filter assay. The membrane was immunostained using the anti-HD1 antibody.

(c) Ultrastructure of a NII. The presence of a NII in a striatal neuron of a 17 month old R6/5 homozygous mouse is shown. The NII is indicated by the large arrow, and the fibrillar amyloid-like structures within the NII are indicated by two small arrows. The scale bar is 250 nm.

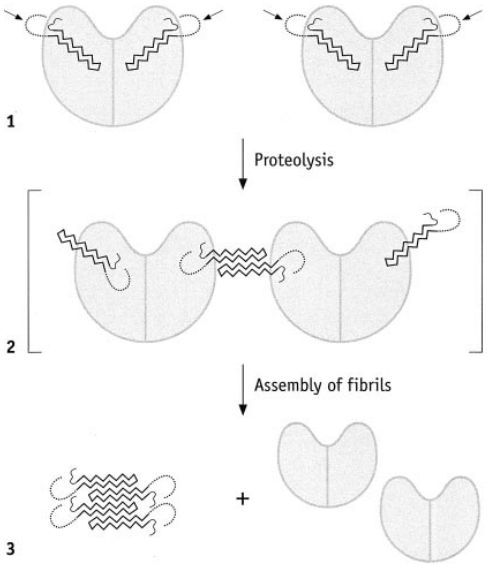

Figure 7. Proposed Mechanism for the Formation of Amyloid-Like Fibrils by Proteolytic Cleavage of GST-HD51

GST-HD51 molecules are represented as follows: zigzag line, elongated polygln repeat forming a stable hairpin with β-sheet structure; dotted line, N-terminal amino acids in the HD exon 1 protein containing the factor Xa cleavage site (arrow) (undefined structure); thin line, C-terminal amino acids in the HD exon 1 protein (undefined structure); shaded symbol, the dimeric globule-like form of GST.

Prior to cleavage, the HD exon 1 protein is tightly bound to the GST tag, preventing intermolecular interactions (1). Removal of the GST tag with factor Xa renders the polygln repeat accessible, allowing the formation of fibrils as seen by EM (3). During cleavage, intermediate structures form through specific polygln interactions before complete release of the GST tag has occurred (2). These intermediates appear as clots under EM and are frequently seen at the terminals of growing fibrils.

Our studies with the GST-HD fusion proteins containing polygln sequences of varying lengths demonstrate that a certain length of the polygln stretch is necessary for the formation of amyloid-like fibrils in vitro. When the purified fusion proteins were analyzed by SDS–PAGE, insoluble high molecular weight protein aggregates were only detected with the proteins containing 81 and 122 glutamines (Figures 1a and 1b), whereas the protein with 51 glutamines was soluble and no fibrillar structures were detected by electron microscopy (Figure 4a). This indicates that the critical length of the polygln stretch in the fusion proteins leading to the formation of aggregates is greater than 51 glutamines. However, when the GST tag, which is known to enhance the solubility of many proteins (Smith and Johnson, 1988), was cleaved by limited digestion with trypsin, the liberated HD exon 1 protein with 51 glutamines also started to form aggregates (Figure 3a) and the amount of these aggregates increased when the GST tag was totally degraded with trypsin (Figure 3b). This indicates that in the HD exon 1 protein 51 glutamines are sufficient to form aggregates, whereas 20 and 30 glutamines under the same conditions are not. The minimum critical length essential for the development of amyloid-like structures after removal of the GST tag is not known and has to be determined. However, preliminary experiments in our laboratory suggest that the threshold for the formation of HD exon 1 protein aggregates is between 35 and 48 glutamines. This result is strikingly similar to the pathological threshold in HD, SBMA, DRPLA, SCA1, SCA2, and SCA3. In all of these neurodegenerative polygln diseases, unaffected individuals have not been described with a repeat length greater than 40 glutamines. This suggests that the elongation of the polygln repeat beyond a certain length may

lead to a phase change. This could, for example, be a change from random coils to hydrogen-bonded hairpins in the polygln stretch. Perutz (1996) proposed that elongated polyglns might form stable hairpins when the number of glutamines exceeds 41. He suggested that at a certain critical length of the polygln sequence, the loss of entropy during formation of the hairpin may become negligible and the system would then become strongly stabilized by a gain of entropy due to the liberated water molecules. Our experimental results with the GST fusion proteins containing polygln sequences of varying lengths support this hypothesis. However, whether the polygln stretch in GST-HD51 has a hairpin structure is not known. Experiments to determine the crystal structure of this protein are in progress.

A proposed mechanism for the fibril formation induced by proteolytic cleavage of GST-HD51 is shown in Figure 7. Based on the known crystal structure of GST with a C-terminal fusion peptide (Lim et al., 1994) and the fact that the purified GST protein is a dimer, we suppose that native GST-HD51 exists as a dimer with two expanded polygln sequences that form stable hairpins consisting of antiparallel β strands strongly held together by hydrogen bonds between the main chain and the side chain amides. In the native protein, both hairpins are tightly bound to the surface of GST and not accessible for protein–protein interactions with other polygln sequences. As a result of the cleavage with a site-specific protease, both hairpins become accessible and β sheets with hairpins from other cleaved protein molecules are formed. This transient population of intermediates consisting of GST molecules and hairpins leads to the formation of polygln-containing β sheet fibrils and free GST molecules. This model is supported by the finding of potential intermediate structures present on one or both ends of the growing fibrils (Figures 4c and 4d). These clots of varying sizes were not detected when GST-HD51 was digested to completion with trypsin, which totally degrades the GST tag, while they were detectable upon limited digestion, leaving the GST moiety largely intact (Figure 4d). This indicates that these structures are transient intermediates.

A model of the formation of amyloid-like fibrils via transient intermediates is not without precedent. Booth et al. (1997) have shown that amyloidogenic lysosome variants aggregate on heating, unlike the wild-type protein, and that the lysozyme fibrils are formed from potential precursor proteins. It is possible that the transient GST-HD intermediates function as nuclei for ordered protein aggregation, very similarly to protein crystallization and microtubule formation, which are nucleation-dependent polymerizations (Jarrett and Lansbury, 1993). Once a nucleus is formed, the further addition of monomers becomes thermodynamically favorable and results in rapid polymerization. An important feature of a nucleation-dependent process is a lag time before the aggregates are detectable. During this period, dimers and trimers are formed. Figure 3a shows that during proteolytic cleavage of GST-HD51, dimers of the released HD portion are formed, the concentration of which then decreases upon prolonged incubation concomitant with an increase in the formation of large protein aggregates (Figure 3b).

For the first time, our results raise the possibility that HD, DRPLA, SBMA, SCA1, SCA2, and SCA3 are the result of a toxic amyloid fibrillogenesis. Although the detection of amyloid-like fibrils has not previously been reported in these inherited diseases, our results strongly suggest that polygln-containing polymers are also formed in vivo by their detection in a transgenic model of polyglutamine disease. The high molecular weight aggregates were exclusively detected in the nuclear fraction prepared from transgene brain material, which is in good agreement with the results of Davies et al. (1997), who demonstrated the presence of the transgene protein and ubiquitin in neuronal intranuclear inclusions, from a time prior to the development of a neurological phenotype. It is likely that the transgene protein is being targeted by ubiquitin for an eventually unsuccessful proteolytic breakdown. The covalent binding of ubiquitin occurs at lysine residues and would not impede polygln interactions. Strikingly, ultrastuctural analysis has shown similar intranuclear inclusions to be present in the cortical and striatal biopsy material from HD patients (Roizin et al., 1979), some of which showed clear evidence of intranuclear fibrils of up to 1 μm in length. More recently, NIIs have been identified in HD post mortem brain material by both immunocytochemistry with N-terminal HD antibodies and electron microscopy (M. DiFiglia, unpublished data). Preliminary experiments in our laboratory with nuclear protein fractions prepared from HD brain material indicated that insoluble huntingtin aggregates are indeed present in these fractions (E. E. Wanker, unpublished data). However, additional control experiments have to be performed to substantiate these results.

One possible explanation for the absence to date of high molecular weight huntingtin protein aggregates in HD brains on immunoblots could be that the aggregates consist mainly of polygln-containing peptides that have been cleaved from the full-length protein. In such a case, only an antibody raised against an N-terminal huntingtin fragment, containing the polgln sequence, would be able to detect the aggregates in the nucleus. In most of the previous immunohistochemical studies, antibodies raised against the central or C-terminal portion of huntingtin have been used, that detect the full-length protein (350 kDa) in the cytosol and in the membrane containing fractions (DiFiglia et al., 1995; Sharp et al., 1995; Trottier et al., 1995a). However, antibodies raised against peptides and fusion proteins from the N and C termini of huntingtin also detected the protein in the nucleus (Hoogeveen et al., 1993; de Rooij et al., 1996), indicating that huntingtin is also present in this subcellular compartment. There are several lines of evidence to implicate a shorter polygln-containing peptide/protein fragment of huntingtin in the pathology of HD. Ikeda et al. (1996) showed that a short fragment of the MJD1 protein containing 79 polyglns (Q79C) but not the full-length protein with the elongated repeat induced apoptotic cell death in COS cells. The polygln-containing protein fragment migrated in SDS gels at a position much higher than expected from its molecular weight, even after boiling in the presence of 2% SDS. These results are in good agreement with our data obtained using the GST-HD fusion proteins containing elongated polygln sequences. Figures 1a and 1b show that the expression

of GST-HD83 and GST-HD122 in E. coli was dramatically reduced compared to the fusion proteins containing 20–51 repeats, and additional studies have indicated that the elongated glutamines are toxic for E. coli cells. Our results confirm the experiments of Onodera et al. (1996), who determined that GST fusion proteins with 59–81 glutamines inhibit both cell growth and protein synthesis in E. coli, whereas the expression of proteins with less than 35–40 glutamines had little or no effect.

The possibility that polygln-containing cleavage products of huntingtin cause neurodegeneration in HD is substantiated by the finding of Goldberg et al. (1996), who showed that an N-terminal 80 kDa huntingtin fragment is cleaved from the full-length protein by apopain, a proapoptotic cysteine protease. This indicates that the N terminus of huntingtin is primarily accessible for proteases and that distinct proteolytic cleavage products can be formed in vitro and in vivo. In addition, there is strong evidence that the mutated huntingtin somehow induces apoptotic cell death in HD, but the underlying molecular mechanism is not known (Duyao et al., 1995; Portera-Cailliau et al., 1995). Our data suggest that a proteolytic cleavage product of huntingtin, which is transported into the nucleus by an unknown mechanism, causes selective neuronal cell death by the formation of insoluble amyloid-like fibrils. It is possibile that the transport to the nucleus is facilitated by a specific nuclear transport mechanism that is unique to certain neuronal cells and involves abnormal protein–protein interactions related to the elongated polygln. Alternatively, there may be specific nuclear proteins in the affected neurons that enhance the huntingtin protein aggregation.

The development of our in vitro model utilizing the GST-HD fusion proteins could potentially open up new avenues for therapeutic interventions. In the event that the formation of polygln-containing amyloid-like fibrils proves to be the cause of HD, an inhibition of this process either directly or indirectly should prevent neuronal cell death. The in vitro system allows the basic screening of a large number of potential therapeutic molecules and should enable us to isolate specific agents that inhibit the formation of polygln-containing polymers. The ability of potential therapeutic agents arising from this screen to prevent neuronal dysfunction and cell death could then be tested in the HD animal model.

Experimental Procedures

Plasmid Construction

Lambda phage from stock 9197_4 (Sathasivam et al., 1997) were plated to give single plaques that were inoculated into 400 ml cultures of E. coli XL1-Blue MRF′ (Stratagene) for DNA preparation. The DNA sequence encoding the N-terminal portion of huntingtin (exon 1), including the CAG repeats, was amplified by PCR using the following pair of primers: ES 25 (TGGGATCCGCATGGCGACCCT GGAAAAGCTGATGAAGG), corresponding to nt 315–343 of the *HD* gene (Huntington's Disease Collaborative Research Group, 1993) and containing a BamHI site (underlined), and ES 26 (GGAGTCGACT CACGGTCGGTGCAGCGGCTCCTCAGC), corresponding to nt 516–588 and containing a SalI site (underlined). Conditions for PCR were as described (Mangiarini et al., 1996). Due to instabiltity of the CAG repeat during propagation in E. coli, DNA preparations from individual plaques yielded different sized PCR products. Fragments of ~320, 360, 480, and 590 bp were gel-purified, digested with BamHI and SalI, and inserted into the BamHI–SalI site of the expression vector pGEX-5X-1 (Pharmacia), yielding pCAG30, pCAG51, pCAG83, and pCAG122, respectively. pCAG20, containing 20 repeats of CAG within the cloned *HD* exon 1 sequence, was similarly constructed from a phage genomic clone derived from a normal allele. All constructs were verified by sequencing.

Purification of GST Fusion Proteins

E. coli SCS1 (Stratagene) carrying the pGEX expression plasmid of interest was grown to an OD_{600} of 0.6 and induced with IPTG (1 mM) for 3.5 hr as described in the manufacturer's protocol (Pharmacia). Cultures (200 ml) of induced bacteria were centrifuged at 4000 g for 20 min, and the resulting pellets were stored at −80°C. Cells were thawed on ice and resuspended in 5 ml of lysis buffer (50 mM sodium phosphate, 150 mM NaCl, 1 mM EDTA [pH 7.4]) containing 0.5 mg/ml lysozyme. After 45 min at 0°C, cells were sonicated with two 30-sec bursts. Octyl-β-D-glucopyranoside was then added to a final concentration of 0.1% and the resulting lysate was clarified by centrifugation at 30,000 g for 30 min at 4°C. Cleared lysates were incubated for 1 hr at 4°C with 500 μl of 1:1 slurry of glutathione-agarose beads (Sigma) that had been washed three times and resuspended in lysis buffer. The beads were poured into a small column and washed extensively with lysis buffer containing 0.1% octyl-β-D-glucopyranoside. The bound fusion protein was eluted with 2 ml of 15 mM glutathione (reduced) in lysis buffer. Typical yields were 0.5–1 mg of purified GST-HD20, -HD30, and -HD51 proteins per 200 ml of bacterial culture; yields of GST-HD83 and -HD122 were much lower, less than 10% of that obtained with the shorter fusion proteins. Protein was determined by the Bio-Rad dye binding assay using bovine serum albumin as standard.

Antibodies and Immunoblotting

A bacterial plasmid encoding HD1-His, a His_6-tagged fusion protein containing residues 1–222 of huntingtin, was generated by inserting a PCR-amplified *IT-15* cDNA fragment into the pQE-32 vector (Qiagen). The fusion protein was expressed in E. coli, affinity-purified under denaturating conditions on Ni-NTA agarose, and injected into rabbits. The resulting immune serum was then affinity-purified against the antigen that had been immobilized on Ni-NTA agarose. The GAPDH- and Fos B–specific antisera have been described (Davies et al., 1997; Wanker et al., 1997).

Western blotting was performed as detailed (Towbin et al., 1979). The blots were incubated with 1:1000 dilutions of the indicated primary antibody, followed by an alkaline-phosphatase-conjugated secondary antibody. Color development was carried out with 5-bromo-4-chloro-3-indolyl phosphate and nitroblue tetrazolium as substrates (Promega).

Site-Specific Cleavage of Fusion Proteins

The GST-HD fusion proteins purified as described above were dialyzed against 40 mM Tris–HCl (pH 8.0), 150 mM NaCl, 0.1 mM EDTA, and 5% (v/v) glycerol to raise the pH prior to proteolytic cleavage. The proteins were then combined with bovine factor Xa (New England Biolabs) or modified trypsin (Boehringer Mannheim, sequencing grade) in dialysis buffer containing 2 mM $CaCl_2$ at an enzyme:substrate ratio of 1:10 (w/w) or 1:40 (w/w), respectively. Incubations with factor Xa were at 25°C for 16 hr. Tryptic digestions were performed at 37°C for 3 or 16 hr as indicated. Digestions were terminated by the addition of PMSF to 1 mM. The degree of proteolysis was determined by SDS–PAGE followed by staining with Coomassie blue or immunoblotting using anti-HD1 antibody.

Filter Retardation Assay

Factor Xa or trypsin digestions of purified GST-HD fusion proteins (10 μg) were performed in a 20 μl reaction mixture as described above. Reactions were terminated by adjusting the mixture to 2% SDS and 50 mM DTT. After heating at 100°C for 5 min, aliquots (0.5 μl) were diluted into 200 μl of 0.1% SDS and filtered through a cellulose acetate membrane (Schleicher and Schuell, 0.2 μm pore size) using a BRL dot blot filtration unit. Filters were washed with water, and the SDS-insoluble aggregates retained on the filter detected by incubation with the anti-HD1 antibody, followed by an anti-rabbit secondary antibody conjugated to alkaline phosphatase

(Boehringer Mannheim). This assay was also used to detect huntingtin aggregates present in a nuclear fraction from the brain of an R6/2 hemizygous mouse and littermate control (see preparation of nuclei below).

Microscopic Analysis of Fusion Proteins

For electron microscopic observation, the native or protease-digested GST-HD fusion proteins were adjusted to a final concentration of 50 μg/ml in 40 mM Tris–HCl (pH 8.0), 150 mM NaCl, 0.1 mM EDTA, and 5% glycerol. Samples were negatively stained with 1% uranyl acetate and viewed in a Philips CM100 EM.

For light microscopy, peptide aggregates formed by trypsin digestion of purified GST-HD fusion proteins (50 μg in 100 μl of digestion buffer) were collected by centrifugation at 30,000 g for 1 hr and resuspended in 10 μl of water. Samples were mixed with 0.1 volume of a 2% (w/v) aqueous Congo Red (Sigma) solution, placed on aminoalkylsilane-coated glass slides, and allowed to dry overnight under a coverslip. After removing the coverslip, excess Congo Red was removed by washing with 90% ethanol. Evaluation of the Congo Red staining by polarization microscopy was performed using a Zeiss Axiolab Pol microscope equipped with strain-free lenses and optimally aligned cross-polarizers.

Preparation of Nuclei

Nuclei from the brain or kidney of an R6/2 hemizygous mouse with a repeat expansion of $(CAG)_{143}$ (Mangiarini et al., 1996) at ten weeks of age and littermate control were prepared as follows. Whole brain samples (80 mg) in 400 μl of 0.25 M sucrose in buffer A (50 mM triethanolamine [pH 7.5], 25 mM KCl, 5 mM $MgCl_2$, 0.5 mM DTT, 0.5 mM PMSF) were homogenized using 15 strokes of a tight-fitting glass homogenizer. The homogenate was adjusted to a final concentration of 5 mM DTT and centrifuged at 800 g for 15 min. The supernatant was recentrifuged at 100,000 g for 1 hr, and the supernatant from this centrifugation was taken as the cytosolic fraction (fraction C). The loose pellet from the first centrifugation was homogenized, diluted to 1.2 ml with 0.25 M sucrose/buffer A, and mixed with two volumes of 2.3 M sucrose/buffer A. The mixture was then layered on top of 0.6 ml of 2.3 M sucrose/buffer A in a SW60 tube and centrifuged at 124,000 g for 1 hr. The pellet was harvested with a spatula, resuspended in 200 μl of 0.25 M sucrose/buffer A, and again centrifuged at 800 g for 15 min. The entire procedure was carried out at 4°C. The pelleted nuclei were resuspended to a density of $\sim 4 \times 10^7$ nuclei/ml in 0.25 sucrose/buffer A (fraction N) and stored at −80°C. Nuclei from mouse kidney were prepared in the same way.

Tissue Processing for Electron Microscopy

A 17 month old R6/5 homozygous mouse [$(CAG)_{128–155}$] (Mangiarini et al., 1996) was deeply anaesthetized with sodium pentobarbitone and then perfused through the left cardiac ventricle with 35–50 ml of 4% paraformaldehyde and either 0.5% glutaraldehyde in 0.1 M Millonig's phosphate buffer (pH 7.4). The brain was removed from the skull and placed in fresh fixative overnight at 4°C. Coronal sections (50–200 μm) were cut on an Oxford Vibratome (Lancer) and collected in serial order in 0.1 M phosphate buffer. After being osmicated (30 min in 1% OsO_4 in 0.1 M phosphate buffer), the sections were stained for 15 min in 0.1 % uranyl acetate in sodium acetate buffer at 4°C, dehydrated in ethanols, cleared in propylene oxide, and embedded in Araldite between two sheets of Melanex (ICI). Semithin (1 μm) sections were cut with glass knives and stained with toluidine blue adjacent to thin sections cut with a diamond knife on a Reichert Ultracut ultramicrotome. The sections were collected on mesh grids coated with a thin formvar film, counterstained with lead citrate, and viewed in a Jeol 1010 electron microscope.

Acknowledgments

Correspondence regarding this paper should be addressed to E. E. W. (e-mail: Wanker@mpimg-berlin-dahlem.mpg.de). We thank N. Wedemeyer, M. Perutz, and S. Schnögl for reading the manuscript and for helpful comments, and A. Mahal for genotyping the mice. The project was funded by the Deutsche Forschungsgemeinschaft grant "Huntingtin and MJD1" and grants from the European Community, Hereditary Disease Foundation, Medical Research Council, and Special Trustees of Guy's and St. Thomas's Hopitals.

Received June 2, 1997; revised July 18, 1997.

References

Bates, G.P., Mangiarini, L., Mahal, A., and Davies, S.W. (1997). Transgenic models of Huntington's disease. Hum. Mol. Genet., in press.

Booth, D.R., Stunde, M., Bellotti, V., Robinson, C.V., Hutchinson, W.L., Fraser, P.E., Hawkins, P.N., Dobson, C.M., Radford, S.E., Blake, C.C.F., and Pepys, M.B. (1997). Instability, unfolding and aggregation of human lysozyme variants underlying amyloid fibrillogenesis. Nature *385*, 787–793.

Burke, J.R., Enghild, J.J., Martin, M.E., Jou, Y.-S., Myers, R.M., Roses, A.D., Vance, J.M., and Strittmatter, W.J. (1996). Huntingtin and DRPLA proteins selectively interact with the enzyme GAPDH. Nat. Med. *2*, 347–350.

Caputo, C.B., Fraser, P.E., Sobel, I.E., and Krischner, D.A. (1992). Amyloid-like properties of a synthetic peptide corresponding to the carboxy terminus of β-amyloid protein precursor. Arch. Biochem. Biophys. *292*, 199–205.

Caughey, B., and Chesebro, B. (1997). Prion protein and the transmissible spongiform encephalopathies. Trends Cell Biol. *7*, 56–62.

Davies, S.W., Trumaine, M., Cozens, B.A., DiFiglia, M., Sharp, A.H., Ross, C.A., Scherzinger, E., Wanker, E.E., Mangiarini, L., and Bates, G.P. (1997). Formation of neuronal intranuclear inclusions (NII) underlies the neurological dysfunction in mice transgenic for the HD mutation. Cell, this issue, *90*, 537–548.

de Rooij, K.E., Dorsman, J.C., Smoor, M.A., den Dunnen, J.T., and van Ommen, G.-J.B. (1996). Subcellular localisation of the Huntington's disease gene product in cell lines by immunofluorescence and biochemical subcellular fractionation. Hum. Mol. Genet. *5*, 1093–1099.

DiFiglia, M., Sapp, E., Chase, K., Schwarz, C., Meloni, A., Young, C., Martin, E., Vonstattel, J.-P., Carraway, R., Reeves, S.A., Boyce, F.M., and Aronin, N. (1995). Huntingtin is a cytoplasmic protein associated with vesicles in human and rat brain neurons. Neuron *14*, 1075–1081.

Duyao, M.P., Auerbach, A.A., Ryan, A., Persichetti, F., Barnes, G.T., McNeil, S.M., Ge, P., Vonstattel, J.-P., Gusella, J.F., Joyner, A.L., and MacDonald, M.E. (1995). Inactivation of the mouse Huntington's disease gene homolog *Hdh*. Science *269*, 407–410.

Glenner, G.G. (1980). Amyloid deposits and amyloidosis. N. Engl. J. Med. *302*, 1283–1292.

Goldberg, Y.P., Nicholson, D.W., Rasper, D.M., Kalchman, M.A., Koide, H.B., Graham, R.K., Bromm, M., Kazemi-Esfarjani, P., Thornberry, N.A., Vaillancourt, J.P., and Hayden, M.R. (1996). Cleavage of huntingtin by apopain, a proapoptotic cysteine protease, is modulated by the polyglutamine tract. Nat. Genet. *13*, 442–449.

Gutekunst, C.-A., Levey, A.I., Heilman, C.J., Whaley, W.L., Yi, H., Nash, N.R., Rees, H.D., Madden, J.J., and Hersch, S.M. (1995). Identification and localization of huntingtin in brain and human lymphoblastoid cell lines with anti-fusion protein antibodies. Proc. Natl. Acad. Sci. USA *92*, 8710–8714.

Harper, P.S. (1991). Huntington's disease, Edition 22, P.S. Harper, ed. (London: W.B. Saunders Co., Ltd).

The Huntington's Disease Collaborative Research Group. (1993). A novel gene containing a trinucleotide repeat that is unstable on Huntington's disease chromosomes. Cell *72*, 971–983.

Hoogeveen, A.T., Willemsen, R., Meyer, N., de Rooij, K.E., Roos, R.A.C., van Ommen, G.-J.B., and Galjaard, H. (1993). Characterisation and localisation of the Huntington disease gene product. Hum. Mol. Genet. *2*, 2069–2073.

Ikeda, H., Yamaguchi, M., Sugai, S., Aze, Y., Narumiya, S., and Kakizuka, A. (1996). Expanded polyglutamine in the Machado-Joseph disease protein induces cell death in vitro and in vivo. Nat. Genet. *13*, 196–202.

Jarrett, J.T., and Lansburry, P.T. (1993). Seeding ''one-dimensional-crystallization'' of amyloid: a pathogenic mechanism in Alzheimer's disease and scrapie? Cell *73*, 1055–1058.

Kalchman, M.A., Graham, R.K., Xia, G., Koide, H.B., Hodgson, J.G., Graham, K.C., Goldberg, Y.P., Gietz, R.D., Pickart, C.M., and Hayden, M.R. (1996). Huntingtin is ubiquinated and interacts with a specific ubiquitin-conjugating enzyme. J. Biol. Chem. *271*, 19385–19394.

Kalchman, M.A., Koide, H.B., McCutcheon, K., Graham, R.K., Nichol, K., Nishiyama, K., Kazemi-Esfariani, P., Lynn, F.C., Wellington, C., Metzler, M., et al. (1997). *HIP1*, a human homologue of *S. cerevisiae* Sla2p, interacts with membrane-associated huntingtin in the brain. Nat. Genet. *16*, 44–53.

Li, X.-J., Li, S.-H., Sharp, A.H., Nucifora, F.C., Schilling, G., Lanahan, A., Worley, P., Snyder, S.H., and Ross, C.A. (1995). A huntingtin-associated protein enriched in brain with implications for pathology. Nature *378*, 398–402.

Lim, K., Ho, J.X., Keeling, K., Gilliland, G.L., Ji, X., Rüker, F., and Carter, D.C. (1994). Three-dimensional structure of Schistosoma japonicum glutamine S-transferase fused with a six-amino acid conserved neutralizing epitope of gp41 from HIV. Prot. Sci. *3*, 2233–2244.

Mangiarini, L., Sathasivam, K., Seller, M., Cozens, B., Harper, A., Hetherington, C., Lawton, M., Trottier, Y., Lehrach, H., Davies, S.W., and Bates, G.P. (1996). Exon 1 of the Huntington's disease gene containing a highly expanded CAG repeat is sufficient to cause a progressive neurological phenotype in transgenic mice. Cell *87*, 493–506.

Onodera, O., Roses, A.D., Tsuji, S., Vance, J.M., Stritmatter, W.J., and Burke, J.R. (1996). Toxicity of expanded polyglutamine-domain proteins in *Escherichia coli*. FEBS Lett. *399*, 135–139.

Perutz, M.F. (1996). Glutamine repeats and inherited neurodegenerative diseases: molecular aspects. Curr. Opin. Struct. Biol. *6*, 848–858.

Perutz, M.F., Johnston, T., Suzuki, M., and Finch, J.T. (1994). Glutamine repeats as polar zippers: their possible role in neurodegenerative diseases. Proc. Natl. Acad. Sci. USA *91*, 5355–5358.

Portera-Cailliau, C., Hedreen, J.C., Price, D.L., and Koliatsos, V.E. (1995). Evidence of apoptotic cell death in Huntington disease and excitotoxic animal models. J. Neurosci. *15*, 3775–3787.

Prusiner, S.B., Kinley, M.P.M., Bowman, K.A., Bolton, D.C., Bendheim, P.E., Groth, D.F., and Glenner, G.G. (1983). Scrapie prions aggregate to form amyloid-like birefingent rods. Cell *35*, 349–358.

Roizin, L., Stellar, S., and Liu, J.C. (1979). Neuronal nuclear-cytoplasmic changes in Huntington's chorea: electron microscope investigations. Adv. Neurol. *23*, 95–122.

Roos, R.A.C., and Bots, G.T.A.M. (1983). Nuclear membrane indentations in Huntington's chorea. J. Neurol. Sci. *61*, 37–47.

Ross, C.A. (1995). When more is less: pathogenesis of glutamine repeat neurodegenerative diseases. Neuron *15*, 493–496.

Rubinsztein, D.C., Leggo, J., Coles, R., Almqvist, E., Biancalana, V., Cassiman, J.-J., Chotai, K., Connarty, M., Crauford, D., Curtis, A., et al. (1996). Phenotypic characterisation of individuals with 30–40 CAG repeats in the Huntington's disease (HD) gene reveals HD cases with 36 repeats and apparently normal elderly individuals with 36–39 repeats. Am. J. Hum. Genet. *59*, 16–22.

Sathasivam, K., Amaechi, I., Mangiarini, L., and Bates, G.P. (1997). Identification of an HD patient with a (CAG)180 repeat expansion and the propagation of highly expanded CAG repeats in lambda phage. Hum Genet. *99*, 692–695.

Sharp, A.H., Loev, S.J., Schilling, G., Li, S.-H., Li, X.-J., Bao, J., Wagster, M.V., Kotzuk, J.A., Steiner, J.P., Lo, A., et al. (1995). Widespread expression of Huntington's disease gene (IT15) protein product. Neuron *14*, 1065–1074.

Smith, D.B., and Johnson, K.S. (1988). Single-step purification of peptides expressed in *Escherichia coli* as fusions with glutathione S-transferase. Gene *67*, 31–40.

Stott, K., Blackburn, J.M., Butler, P.J.G., and Perutz, M. (1995). Incorporation of glutamine repeats makes protein oligomerize: implications for neurodegenerative diseases. Proc. Natl. Acad. Sci. USA *92*, 6509–6513.

Tellez-Nagel, I., Johnson, B., and Terry, R.D. (1974). Studies on brain biopsies of patients with Huntington's chorea. J. Neurocyt. *3*, 308–332.

Towbin, H., Staehelin, T., and Gordon, J. (1979). Electrophoretic transfer of proteins from polyacrylamide gels to nitrocellulose sheets: procedure and some applications. Proc. Natl. Acad. Sci. USA *76*, 4350–4354.

Trottier, Y., Devys, D., Imbert, G., Sandou, F., An, I., Lutz, Y., Weber, C., Agid, Y., Hirsch, E.C., and Mandel, J.-L. (1995a). Cellular localisation of the Huntington's disease protein and discrimination of the normal and mutated forms. Nat. Genet. *10*, 104–110.

Trottier, Y., Lutz, Y., Stevanin, G., Imbert, G., Devys, D., Cancel, G., Sandou, F., Weber, C., David, G., Tora, L., et al. (1995b). Polyglutamine expansion as a pathological epitope in Huntington's disease and four dominant cerebellar ataxias. Nature *378*, 403–406.

Vonsattel, J.-P., Myers, R.H., Stevens, T.J., Ferrante, R.J., Bird, E.D., and Richardson, E.P. (1985). Neuropathological classification of Huntington's disease. J. Neuropath. Exp. Neurol. *44*, 559–577.

Wanker, E.E., Rovira, C., Scherzinger, E., Hasenbank, R., Walter, S., Tait, D., Colicelli, J., and Lehrach, H. (1997). HIP-1: a huntingtin interacting protein isolated by the yeast two-hybrid system. Hum. Mol. Genet. *6*, 487–495.